Extending Sommerfeld integral based spherical wavefield computations beyond two layers

Arnim B. Haase

ABSTRACT

Plane-wave theory is the commonly accepted approach to AVO-analysis/inversion but it is known to break down near critical angles and at large offsets. What is more, commonly employed linear approximations to Zoeppritz's equations make the assumption of small parameter changes across the interface. Large offsets are desirable, however, when estimating densities by AVO-inversion. Spherical-wave theory overcomes offset related and small parameter change problems, but does not account for reverberations and tuning when only one interface is considered. In order to bring AVO and VSP modelling closer to actual geology, an extension to multi-layer situations is introduced. Based on the Ewing-method, multi-layer boundary equations are developed and programmed. Computed plane-wave reflection and transmission coefficients are then applied in Sommerfeld integrals to obtain multi-layer spherical-wave responses. A three-layer P-wave example modelled with this technique shows the expected reverberations and spherical spreading.

INTRODUCTION

AVO-analysis has experienced ever increasing popularity from the time it was introduced by Ostrander (1984). Most of these developments are based on plane-wave analysis. Spherical-wave analysis results depart from plane-wave comparisons at larger offsets beyond approximately 30° of incidence angle (Haase and Ursenbach, 2006). Large offsets are desirable when estimating densities by AVO-inversion. Downton and Lines (2002) investigate normal moveout correction as an AVO error source when working with seismic data. Residual moveout (RNMO) is not a problem in modelling studies where velocities are known exactly. There is, however, a potential error source because of a common simplification. All the computational AVO model investigations undertaken in previous years by this author are based on two-layer/one-interface assumptions. Note that also the Zoeppritz equations are derived for "*one interface*" situations. Reservoirs in the real world are of finite thickness. Therefore it seems more appropriate to model the three-layer case with two interfaces. It is the aim of this study to develop algorithms for multi-layer model computations that can also be simplified to three-layer situations. There are, of course, other applications for multi-layer modelling techniques that go beyond AVO-analysis. One such field is VSP modelling which will be addressed in a future study.

THEORY

When deriving elastic/anelastic spherical-wave displacement reflection/transmission coefficients for single interface situations by assuming continuity of displacement and stress across a boundary in welded contact (Haase and Ursenbach, 2006) these coefficients are found to be scaled versions of plane-wave reflection/transmission coefficients derived from Zoeppritz's equations (Aki and Richards, 1980). Because those derivations are already tedious in single interface situations a computational approach is

desirable for more complicated multi-layer cases. The problem of a point source in a layered half space is addressed by Ewing et al. (1957). For each layer *j*, Ewing et al. calculate the potentials φ_j and ψ_j as a sum of two Sommerfeld integrals (using their notation):

$$\varphi_j = \int_0^\infty Q_j^{'} J_0(kr) e^{-\nu_j z} dk + \int_0^\infty Q_j^{''} J_0(kr) e^{\nu_j z} dk \quad , \tag{1a}$$

$$\psi_j = \int_0^\infty S_j^{'} J_0(kr) e^{-\nu_j^{'} z} dk + \int_0^\infty S_j^{''} J_0(kr) e^{\nu_j^{'} z} dk \quad , \tag{1b}$$

where Q and S are as yet unknown coefficients.

These unknown coefficients can be found by solving the system of equations for all layers determined by all boundary conditions. The first integral in both equations computes the down-going wave-field in Layer *j*, one frequency point at a time; similarly, the second integral computes the up-going wave-field in Layer *j*. This is the sought after computational approach. From Haase and Ursenbach (2006) we know that Q and S consist of scaling factors and plane-wave reflection/transmission coefficients derived from Zoeppritz's equations. We will introduce the known scale factors directly into the Sommerfeld integrals below and compute all reflection/transmission coefficients from the boundary conditions at all interfaces. For the first interface we conveniently set the depth z_1 to zero giving us the four Zoeppritz equations from the boundary conditions at the first interface plus two delayed terms representing P-wave reflections and S-wave reflections from the next (second) interface below located at z_2:

$$A_{R1}\alpha_1 p + B_{R1}\beta_1\eta_1 - (A_{T1} + A_{R2}e^{-i\omega\xi_2 z_2})\alpha_2 p - (B_{T1} + B_{R2}e^{-i\omega\eta_2 z_2})\beta_2\eta_2 = -A_{I1}\alpha_1 p \quad , \tag{2a}$$

$$-A_{R1}\alpha_1\xi_1 + B_{R1}\beta_1 p - (A_{T1} - A_{R2}e^{-i\omega\xi_2 z_2})\alpha_2\xi_2 + (B_{T1} - B_{R2}e^{-i\omega\eta_2 z_2})\beta_2 p = -A_{I1}\alpha_1\xi_1 \quad , \tag{2b}$$

$$-2A_{R1}\alpha_1\beta_1^2\rho_1 p\xi_1 - B_{R1}\beta_1\rho_1(1-2\beta_1^2 p^2) - (A_{T1} - A_{R2}e^{-i\omega\xi_2 z_2})2\alpha_2\beta_2^2\rho_2 p\xi_2 - (B_{T1} - B_{R2}e^{-i\omega\eta_2 z_2})\beta_2\rho_2(1-2\beta_2^2 p^2) = -2A_{I1}\alpha_1\beta_1^2\rho_1 p\xi_1 \quad , \tag{2c}$$

$$A_{R1}\alpha_1\rho_1(1-2\beta_1^2 p^2) - 2B_{R1}\beta_1^3\rho_1 p\eta_1 - (A_{T1} + A_{R2}e^{-i\omega\xi_2 z_2})\alpha_2\rho_2(1-2\beta_2^2 p^2) + (B_{T1} + B_{R2}e^{-i\omega\eta_2 z_2})2\beta_2^3\rho_2 p\eta_2 = -A_{I1}\alpha_1\rho_1(1-2\beta_1^2 p^2) \quad , \tag{2d}$$

where A_{Rj} is the P-wave reflected from interface *j*,

B_{Rj} is the S-wave reflected from interface *j* (or converted on reflection),

A_{Tj} is the P-wave transmitted through interface *j*,

B_{Tj} is the S-wave transmitted through interface *j* (or converted on transmission),

α_k and β_k are P-wave and S-wave velocities of Layer *k*,

ξ_k and η_k are vertical P-wave and S-wave slownesses of Layer k,

ρ_k is the density of Layer k,

p is the horizontal slowness and

ω is the frequency.

A_{I1} represents the P-wave incident on the first interface and is given by the source wavelet. Incident on the second and subsequent interfaces are the P-waves (A_{Tj}) and S-waves (B_{Tj}) transmitted (or converted on transmission) through the interface immediately above. Thus we obtain for the second interface at a non-zero depth z2

$$e^{-i\omega\xi_2 z_2}(A_{T1}+A_{R2})\alpha_2 p+e^{-i\omega\eta_2 z_2}(B_{T1}+B_{R2})\beta_2\eta_2 \qquad (3a)$$
$$-e^{-i\omega\xi_2 z_2}(A_{T2}+A_{R3}e^{-i\omega\xi_3(z_3-z_2)})\alpha_3 p-e^{-i\omega\eta_2 z_2}(B_{T2}+B_{R3}e^{-i\omega\eta_3(z_3-z_2)})\beta_3\eta_3=0\ ,$$

$$e^{-i\omega\xi_2 z_2}(A_{T1}-A_{R2})\alpha_2\xi_2-e^{-i\omega\eta_2 z_2}(B_{T1}-B_{R2})\beta_2 p \qquad (3b)$$
$$-e^{-i\omega\xi_2 z_2}(A_{T2}-A_{R3}e^{-i\omega\xi_3(z_3-z_2)})\alpha_3\xi_3-e^{-i\omega\eta_2 z_2}(B_{T2}-B_{R3}e^{-i\omega\eta_3(z_3-z_2)})\beta_3 p=0\ ,$$

$$2e^{-i\omega\xi_2 z_2}(A_{T1}-A_{R2})\alpha_2\beta_2^2\rho_2\xi_2 p+e^{-i\omega\eta_2 z_2}(B_{T1}-B_{R2})\beta_2\rho_2(1-2\beta_2^2p^2) \qquad (3c)$$
$$-e^{-i\omega\xi_2 z_2}(A_{T2}-A_{R3}e^{-i\omega\xi_3(z_3-z_2)})2\alpha_3\beta_3^2\rho_3\xi_3 p-e^{-i\omega\eta_2 z_2}(B_{T2}-B_{R3}e^{-i\omega\eta_3(z_3-z_2)})\beta_3\rho_3(1-2\beta_3^2p^2)=0\,,$$

$$e^{-i\omega\xi_2 z_2}(A_{T1}+A_{R2})\alpha_2\rho_2(1-2\beta_2^2p^2)-e^{-i\omega\eta_2 z_2}(B_{T1}+B_{R2})2\beta_2^3\rho_2\eta_2 p \qquad (3d)$$
$$-e^{-i\omega\xi_2 z_2}(A_{T2}+A_{R3}e^{-i\omega\xi_3(z_3-z_2)})\alpha_3\rho_3(1-2\beta_3^2p^2)+e^{-i\omega\eta_2 z_2}(B_{T2}+B_{R3}e^{-i\omega\eta_3(z_3-z_2)})2\beta_3^3\rho_3\eta_3 p=0\,.$$

Similar equations can be derived for all subsequent interfaces (except the last) by accumulating appropriate travel times (layer thickness Δz_k multiplied by vertical layer slownesses ξ_k or η_k) according to

$$e^{-i\omega\sum_{k=1}^{j}(\xi_k\,\Delta z_k)} \quad \text{and} \quad e^{-i\omega\sum_{k=1}^{j}(\eta_k\,\Delta z_k)} \qquad (4)$$

as well as changing subscripts. For the last interface there is no reflected wave from below.

Every interface has four equations for four unknowns. Because variables are "*borrowed*" from neighbouring interfaces a system of equations must be solved. Plane-wave reflection and transmission coefficients for all interfaces are obtained by elimination and back-substitution. These plane-wave coefficients are then used in Sommerfeld integrals for the computation of spherical-wave displacements. For the down-going (transmitted) P-wave along the ray in Layer j we evaluate (Haase and Stewart, 2007):

$$u_{pj}(\omega) = i\omega e^{-i\omega t} \int_0^{\infty} T_{j-1}(p) \left[\frac{p^2}{\xi_j} J_1(\omega p r) \sin(\theta_j) - ip J_0(\omega p r) \cos(\theta_j) \right] e^{i\omega \sum_{k=1}^{j} (\Delta z_k \xi_k)} dp \ , \tag{5}$$

where $u_{pj}(\omega)$ is the P-wave displacement along the ray in Layer j at ω,
ω is the frequency in radians,
t is the time,
j is the number of layers between the source and the receiver,
$T_{j-1}(p)$ is the Zoeppritz transmission coefficient from Layer j-1 to Layer j,
p is the horizontal slowness,
ξ_j is the vertical slowness of Layer j,
J_0 and J_1 are zero and first order Bessel functions of the first kind,
r is the range (horizontal offset between source and receivers), and
θ_j is the ray angle in Layer j.

Note that Δz_j is the receiver position in Layer j (as opposed to the layer thickness).The up-going (reflected) P-wave displacement along the ray in Layer j can be computed from Equation 5 by replacing the transmission coefficient $T_{j-1}(p)$ with the reflection coefficient $R_j(p)$ which is the reflection off the bottom of Layer j.

For zero-offset VSP modelling we make the range r a small number (e.g. 1m) and locate VSP-receivers throughout the layers at various depths z. VSP-receivers will always detect up-going (reflected) *and* down-going (direct or transmitted) wave-fields unless the medium is homogeneous.

For AVO modelling all receivers are placed at source elevation in the first layer but at various ranges r. In addition to a direct wave there is only reflected energy in the first layer.

PLANE-WAVE AND SPHERICAL-WAVE TESTS

Equations 2 and 3 show matrix entries for the first two interfaces of a multi-layer system. The right-hand side is non-zero only for the first interface (located between the first and second layer) because the P-wave source is positioned in the first layer. The equations for subsequent matrix entries are similar to Equations 3 but apply the velocities and densities of the layers they represent. In diagonalizing this matrix we compute plane-wave transmission and reflection coefficients. To test this algorithm velocity and density values are changed across one interface at a time (single reflector situation) and the resulting reflection coefficients are compared to Zoeppritz equation computations for the same layer parameter changes. Figure 1 shows a comparison of real and imaginary parts of a P-wave reflection coefficient $R_{pp}(p)$. The rock parameters used are:

$\alpha_1 = 2000$ m/s ,

$\beta_1 = 879.88$ m/s ,

$\rho_1 = 2400$ kg/m^3 ,

$\alpha_2 = 2933.33$ m/s ,

$\beta_2 = 1882.29$ m/s ,

$\rho_2 = 2000$ kg/m^3 ,

which describe a Class 1 AVO anomaly (Haase and Ursenbach, 2006).

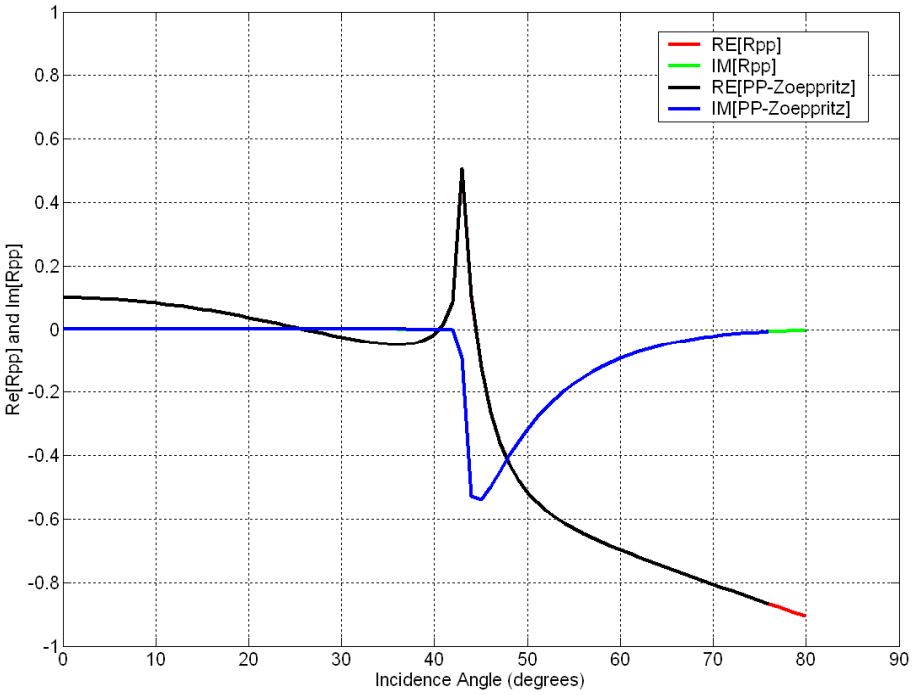

FIG. 1. Real part and imaginary part of plane-wave Class 1 elastic reflection coefficients.

The imaginary part displayed in Figure 1 is non-zero only beyond the critical angle of approximately 43°. This result is the same for all test interface locations chosen. P-wave and C-wave Class 1 AVO-responses for the plane-wave situation are plotted in Figure 2. There is excellent agreement with Zoeppritz computations in both Figures 1 and 2.

The crucial test for this multi-layer algorithm is the step *beyond* single reflector (two-layer) situations where multiples (reverberations) can be expected. The Class1 AVO example above has a zero-offset P-wave reflectivity of only 0.1 and multiple reflections are too weak to be clearly visible on plots. For a *reverberations* test the following layer parameters are chosen:

$\alpha_1 = 2000$ m/s ,

$\beta_1 = 1000$ m/s ,

$\rho_1 = 2400$ kg/m^3 ,

$\alpha_2 = 1000$ m/s ,

$\beta_2 = 500$ m/s ,

$\rho_2 = 1200$ kg/m^3 .

The top of the second layer (the reservoir layer) is at 500 m depth and reservoir thickness is100 m. A third layer (located below the reservoir) is assumed to be the same medium as the top (overburden) layer. P-wave displacements along the ray computed with this three-layer model and a 5/15-80\100 Hz zero-phase (non-causal) Ormsby wavelet (P-wave source) can be seen in Figure 3. The first event at 500 ms is a top of reservoir reflection with negative polarity because of a P-wave velocity inversion. Event number 2 at 700 ms is a reflection off the reservoir bottom with positive polarity caused by a P-wave velocity increase at the second interface. Subsequent events are multiple reflections representing reservoir layer reverberations that are spaced 200 ms apart. This spacing is dictated by an assumed reservoir thickness of 100 m and a reservoir P-wave velocity of 1000 m/s. Note the typical Ormsby wavelet ringing of the first two events. Of interest are also the two far offset traces in Figure 3. Just before 900 ms, approximately halfway between the reservoir bottom reflection and the first multiple, another event with negative polarity is barely visible. The timing suggests a one-way traverse of the reservoir at the S-wave velocity which would mean one conversion on transmission and one conversion on reflection take place.

CONCLUSIONS

Based on the work of Ewing et al. (1957) equations for the computation of point source responses in elastic and anelastic multi-layered media situations are developed. A system of equations is set up by introducing the boundary conditions of all interfaces between the layers. Plane-wave particle motion reflection and transmission coefficients for all interfaces are obtained from the solution of this system. These plane-wave coefficients are then introduced into Sommerfeld integrals for the computation of up-going and down-going spherical-wave displacements. A three-layer/two-interface P-wave example modelled by the resulting Sommerfeld integrals shows the expected reverberations and spherical spreading. There is also evidence of doubly converted energy at large offsets. As a next step in this investigation the Ewing-algorithm is applied to a three-layer spherical-wave AVO situation (Haase, 2008, this Volume). Future work will include three-layer and multi-layer model Q-estimation from synthetic VSP data generated with this method.

ACKNOWLEDGEMENTS

Support from the CREWES Project at the University of Calgary and its industrial sponsorship is gratefully acknowledged.

REFERENCES

Aki, K.T., and Richards, P.G., 1980, Quantitative Seismology: Theory and Methods: Vol. 1, W.H. Freeman and Co.

Downton, J.E., and Lines, L.R., 2002, AVO NMO: CREWES Research Report, Volume 14.
Ewing, W.M., Jardetzky, W.S., and Press, F., 1957, Elastic Waves in Layered Media: McGraw-Hill Book Company, Inc.
Haase, A.B., and Ursenbach, C.P., 2006, Spherical-wave AVO modelling in elastic and anelastic media: CREWES Research Report, Volume 18.
Haase, A.B., and Stewart, R.R., 2007, Testing VSP-based Q-estimation with spherical wave models: CREWES Research Report, Volume 19.
Haase, A.B., 2008, Modelling Class 1 AVO responses of a three layer system: CREWES Research Report, Volume 20.
Ostrander, W.J., 1984, Plane-wave reflection coefficients for gas sands at nonnormal angles of incidence: Geophysics, **49,** 10, 1637-1648.

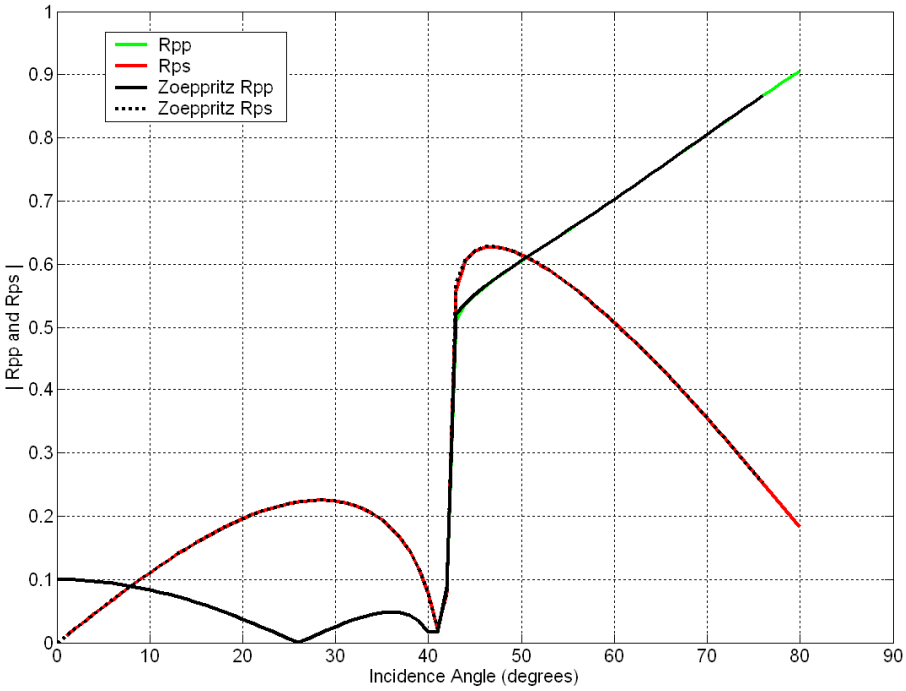

FIG. 2. Plane-wave Class 1 elastic reflection coefficient comparison.

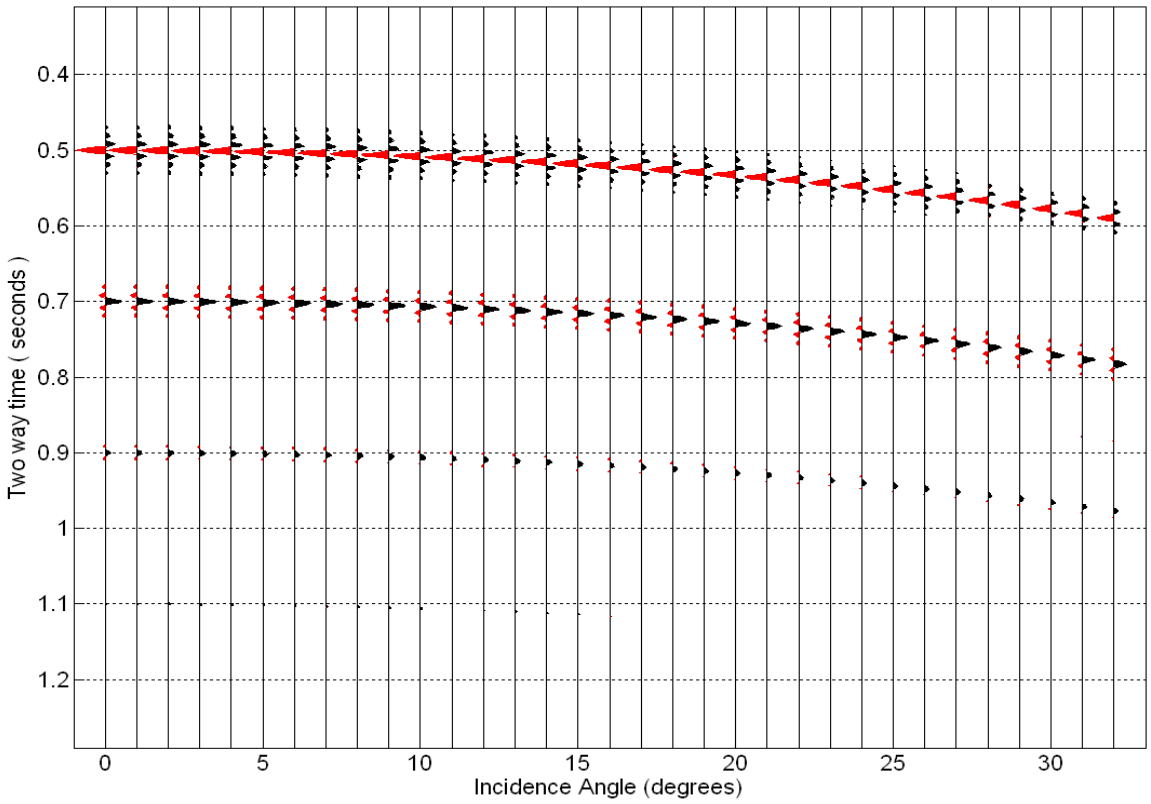

FIG. 3. P-wave multiples (reverberations) of a spherically spreading wave-front generated in a 100 m reservoir (the reservoir top is at 500 m depth). The top-of-reservoir reflection arrives at 500 ms. The event at 700 ms is a reflection off the reservoir bottom and reservoir layer reverberations can be seen below that.